The clathrin adaptor complex 1 directly binds to a sorting signal in Ste13p to reduce the rate of its trafficking to the late endosome of yeast

Christopher Foote and Steven F. Nothwehr

Division of Biological Sciences, University of Missouri, Columbia, MO 65211

Yeast trans-Golgi network (TGN) membrane proteins maintain steady-state localization by constantly cycling to and from endosomes. In this study, we examined the trafficking itinerary and molecular requirements for delivery of a model TGN protein A(F→A)–alkaline phosphatase (ALP) to the prevacuolar/endosomal compartment (PVC). A(F→A)-ALP was found to reach the PVC via early endosomes (EEs) with a half-time of ∼60 min. Delivery of A(F→A)-ALP to the PVC was not dependent on either the GGA or adaptor protein 1 (AP-1) type of clathrin adaptors, which are thought to function in TGN to PVC and TGN to EE transport, respectively. Surprisingly, in cells lacking the function of both GGA and AP-1 adaptors, A(F→A)-ALP transport to the PVC was dramatically accelerated. A 12-residue cytosolic domain motif of A(F→A)-ALP was found to mediate direct binding to AP-1 and was sufficient to slow TGN→EE→PVC trafficking. These results suggest a model in which this novel sorting signal targets A(F→A)-ALP into clathrin/AP-1 vesicles at the EE for retrieval back to the TGN.

Introduction

The enzymes dipeptidyl aminopeptidase A/Ste13p and endopeptidase Kex2p, which process the α-factor mating pheromone in the yeast *Saccharomyces cerevisiae*, undergo repeated cycles of vesicular transport between the TGN and endosomal system (Nothwehr et al., 1993; Brickner and Fuller, 1997; Bryant and Stevens, 1997). These enzymes possess large lumenal domains, a single transmembrane-spanning domain, and cytosolic domains of ∼100 amino acids. Within their trafficking itinerary, the best understood step is retrieval from the prevacuolar/endosomal compartment (PVC) back to the TGN, which is mediated by the retromer, an apparent vesicle coat complex (Seaman, 2005). Retromer recognition of Ste13p and the carboxypeptidase Y receptor Vps10p occurs via binding of the Vps35p retromer subunit with aromatic amino acid–based sorting signals such as FXFXD in Ste13p (Nothwehr et al., 1993, 1999, 2000; Marcusson et al., 1994; Cooper and Stevens, 1996). However, the manner by which Ste13p and Kex2p reach the PVC is poorly understood.

Some studies suggest that Ste13p and Kex2p may traverse via the early endosome (EE) en route to the PVC. A Ste13p-based reporter protein, A(F→A)–alkaline phosphatase (ALP), reaches the PVC slowly with a half-time of ∼60 min, whereas other proteins such as Vps10p and Cps1p reach the PVC within 5–15 min (Bryant and Stevens, 1997; Cowles et al., 1997). Deletion of the 2–11 region within the Ste13p cytosolic domain accelerates trafficking of A(F→A)-ALP into the PVC (Bryant and Stevens, 1997; Ha et al., 2001). A signal analogous to 2–11 exists in Kex2p (Brickner and Fuller, 1997). These data are consistent with a model in which A(F→A)-ALP reaches the PVC via the EE with the 2–11 signal conferring either EE to TGN retrieval or static retention within the TGN/EE. In support of an itinerary involving the EE, the loss of function of a yeast synaptojanin like protein Inp53p/Sjl3p, which is thought to play a role in TGN/EE traffic, accelerates the rate of trafficking of A(F→A)-ALP into the PVC but has no effect on Vps10p trafficking (Ha et al., 2001). In addition, Kex2p has been colocalized with EE markers Tlg1p and chitin synthetase III (Chs3p) as well as Snc1p, a late secretory v-SNARE that recycles from the plasma membrane back to the TGN via an early endosomal compartment (Ziman et al., 1996; Santos and Snyder, 1997; Holthuis et al., 1998; Lewis et al., 2000). Finally, the loss of function of Soi3p, which appears to be required for efficient EE to PVC trafficking, delayed trafficking of a PVC retrieval-defective form of Kex2p to the PVC but did not affect Vps10p trafficking (Sipos et al., 2004).

Clathrin-associated vesicular transport machinery clearly plays a role in trafficking between the TGN and endosomes

Correspondence to Steven F. Nothwehr: nothwehrs@missouri.edu

Abbreviations used in this paper: ALP, alkaline phosphatase; AP-1, adaptor protein 1; EE, early endosome; MBP, maltose-binding protein; PVC, prevacuolar/endosomal compartment.

The Journal of Cell Biology, Vol. 173, No. 4, May 22, 2006 615–626
http://www.jcb.org/cgi/doi/10.1083/jcb.200510161

of yeast. A loss of function in either clathrin heavy chain or Vps1p, a dynamin homologue that is thought to participate in the production of clathrin-coated vesicles, causes Ste13p and Kex2p to be mislocalized to the cell surface (Payne and Schekman, 1989; Seeger and Payne, 1992; Ha et al., 2003). This suggests that there is a requirement for clathrin in both TGN to EE and TGN to PVC pathways. Furthermore, clathrin-coated compartments have been shown to contain Vps10p and Kex2p (Deloche et al., 2001), and clathrin is required for in vitro TGN to PVC trafficking of Kex2p (Abazeed et al., 2005).

Two types of clathrin-associated adaptors function within the yeast TGN/endosomal system. The *GGA1* and *GGA2* gene products (Dell'Angelica et al., 2000; Hirst et al., 2000) are thought to function in the direct TGN to PVC pathway. Loss of GGA function causes the PVC-localized t-SNARE Pep12p to be mislocalized to the EE (Black and Pelham, 2000). Likewise, the delivery of Vps10p to the PVC and Cps1p to the PVC/vacuole, cargoes that are thought to use the direct TGN to PVC pathway, are delayed in *gga1,2Δ* mutants (Costaguta et al., 2001). No delay in A(F→A)-ALP transport into the PVC was observed in a strain lacking GGA function (Ha et al., 2003); however, a moderate delay has been reported for Kex2p (Costaguta et al., 2001). Thus, a role for GGA proteins in the trafficking of TGN resident proteins is still obscure. In contrast to the GGAs, the adaptor protein 1 (AP-1) complex appears to be involved in trafficking between the EE and TGN. Loss of AP-1 function caused the mislocalization of Chs3p to the cell surface under conditions in which it was sequestered to the EE (Valdivia et al., 2002). A severe synthetic growth defect has been observed upon the simultaneous loss of function of the GGA proteins and AP-1 (Costaguta et al., 2001). This synthetic growth defect suggests that both adaptors may mediate anterograde transport into the endosomal system, but this model has not been rigorously tested.

In this study, we tested whether A(F→A)-ALP required the AP-1 complex for transport into the PVC when the GGA-mediated pathway and the plasma membrane route were blocked. We found that when AP-1 complex function was lost under these conditions, the transport of A(F→A)-ALP into the PVC was dramatically accelerated. In addition, we demonstrate that the AP-1 complex interacts with the 2–11 sorting signal within the Ste13p cytosolic domain. These results are most consistent with a model in which clathrin/AP-1 recognizes Ste13p in the EE and directs it into a retrograde pathway to the TGN.

Results

The itinerary of A-ALP includes an EE compartment as well as the PVC

A-ALP is a model TGN membrane protein consisting of the NH_2-terminal cytosolic domain of Ste13p fused to the transmembrane and luminal domains of ALP (Nothwehr et al., 1993). When TGN/endosome retention is perturbed, A-ALP is transported to the vacuole, where its COOH-terminal propeptide is proteolytically removed. For example, mutation of the $FXFXD_{89}$ retromer recognition motif prevents the retrieval of A-ALP from the PVC to the TGN (Bryant and Stevens, 1997; Nothwehr et al., 2000). This mutant, A(F→A)-ALP, is proteolytically processed with a half-time of ~60 min, reflecting the kinetics of vacuolar delivery (Nothwehr et al., 1993). A-ALP has also been shown to reach the PVC in a class E *vps* mutant with similar kinetics (Bryant and Stevens, 1997; Ha et al., 2001), indicating that the PVC to vacuole step is quite rapid and that the rate of A(F→A)-ALP processing largely reflects the rate of trafficking into the PVC.

To test whether the A-ALP itinerary includes EEs, it was tagged with GFP and was expressed using the moderate strength *CYC1* promoter (Mumberg et al., 1995). Like its untagged counterpart, pulse-chase immunoprecipitation analysis of GFP–A-ALP indicated that it was unprocessed after 60 min, whereas mutation of the $FXFXD_{89}$ motif resulted in processing with a half-time of ~60 min (unpublished data). Because the GFP tag did not interfere with the kinetics of transport into the PVC/vacuole, it is likely that the tag did not disrupt the normal trafficking patterns of A-ALP. Consistent with this, GFP–A-ALP exhibited a punctate staining pattern typical of yeast Golgi/endosomal proteins (Fig. 1 A). Cells expressing GFP–A-ALP were incubated at 0°C with the lipophilic dye FM4-64, allowing it to integrate into the plasma membrane but not be internalized (Vida and Emr, 1995). The cells were then incubated at 30°C for 2 min to allow the dye to be transported from the plasma membrane to EEs. After 2 min, FM4-64 exhibited a punctate pattern

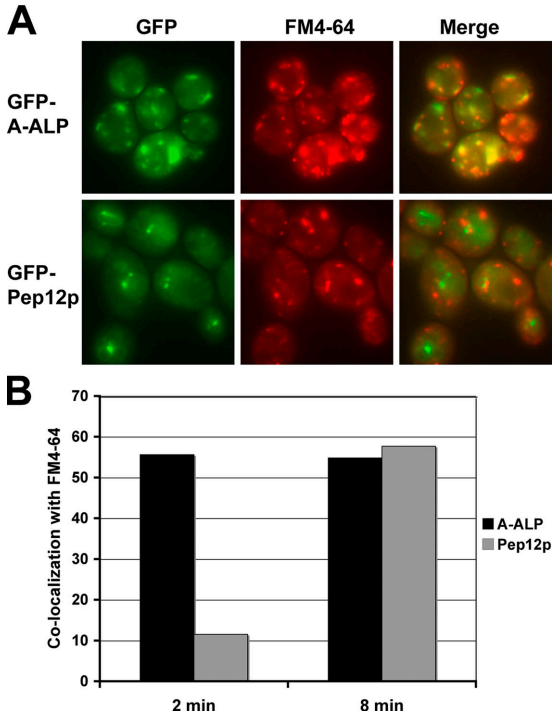

Figure 1. **GFP-tagged A-ALP partially colocalizes with EEs.** Strains SHY35/pCF17 and SHY35/pG-P12-U were stained at 0°C with FM4-64, and the dye was allowed to internalize by incubating in media at 30°C for 2 or 8 min followed by the addition of NaN_3 and NaF to halt traffic. (A) After 2 min of internalization, GFP-ALP, GFP-Pep12p, and FM4-64 were imaged as indicated. (B) The percentage of punctate FM4-64 structures that were positive for either GFP–A-ALP or GFP-Pep12p was quantified after 2 and 8 min of incubation at 30°C. A minimum of 150 punctate structures were analyzed for each data point.

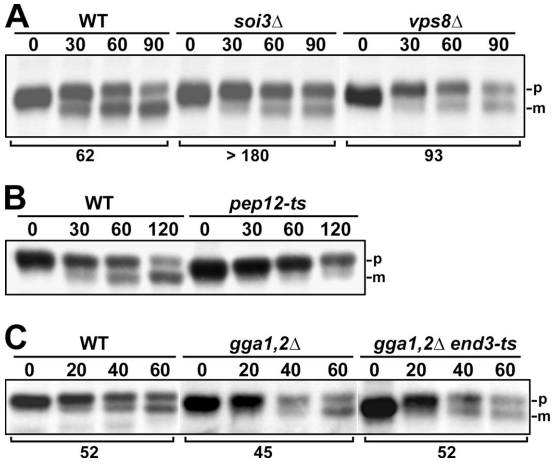

Figure 2. **A(F→A)-ALP uses a TGN→EE→PVC pathway before reaching the vacuole.** Wild-type (SHY35), *soi3Δ* (CFY38), *vps8Δ* (CFY37), *pep 12-49*^{ts} (SNY156), *gga1,2Δ* (SNY165), and *gga1,2Δ end3-ts* (SNY171-4D) strains carrying a plasmid expressing A(F→A)-ALP (pSN100) were analyzed. Cells were pulsed for 10 min with [^{35}S]methionine/cysteine and chased for the indicated times. The strains were either incubated at 30°C throughout the time course (A) or were propagated for several doublings at 24°C before shifting to 36°C for 10 min before initiation of the chase (B and C). After each time point, A(F→A)-ALP was immunoprecipitated and analyzed by SDS-PAGE to separate the precursor (p) and mature (m) forms. The half-time of processing of each strain is indicated below the panels in A and C.

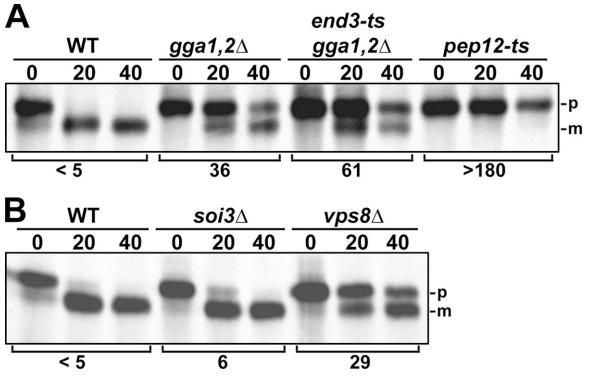

Figure 3. **Cps1p uses a GGA-dependent direct TGN to PVC pathway before reaching the vacuole.** Strains CFY30, CFY32, CFY33, and CFY31 (from left to right) carrying a CEN-*CPS1* plasmid were analyzed in A, whereas strains SHY35, CFY38, and CFY37 were analyzed in B. The strains were either propagated for several doublings at 24°C before shifting to 36°C for 10 min before the initiation of the chase (A) or were incubated at 30°C throughout the time course (B). After each chase time, Cps1p was immunoprecipitated, treated with endoglycosidase H, and analyzed by SDS-PAGE to separate the precursor (p) and mature (m) forms. The half-time of processing of each strain is indicated below each panel.

typical of endosomes with little or no vacuolar or plasma membrane staining (Fig. 1 A). 56% of these FM4-64 structures colocalized with GFP–A-ALP (Fig. 1, A and B). In contrast, 11% of the FM4-64–positive structures contained the GFP-tagged PVC syntaxin Pep12p (Black and Pelham, 2000), indicating that the vast majority are EEs rather than PVCs. After 8 min of internalization, FM4-64 exhibited some vacuolar staining in addition to punctate endosomal staining (unpublished data). Of the FM4-64 punctate structures observed after 8 min of internalization, 55% were positive for GFP–A-ALP, whereas 58% were positive for GFP-Pep12p. These data indicate that a pool of FM4-64 was transported from EEs to PVCs during the intervening 6 min. The significant FM4-64/GFP–A-ALP colocalization at both time points is consistent with A-ALP populating both EEs and PVCs. The minimal FM4-64/GFP-Pep12p colocalization at 2 min would be expected given that its localization is restricted to the PVC (Becherer et al., 1996; Black and Pelham, 2000).

Vps8p and Soi3p are thought to be required for EE to PVC transport (Luo and Chang, 2000; Sipos et al., 2004), whereasVps8p appears to also function in PVC to vacuole trafficking (Subramanian et al., 2004). A(F→A)-ALP processing was clearly slowed in a *soi3Δ* strain and was slowed to a lesser degree in a *vps8Δ* strain (Fig. 2 A). These results indicate that like Kex2p (Sipos et al., 2004), A(F→A)-ALP is transported along an EE to PVC route.

We next tested whether trafficking via the PVC is absolutely necessary for A(F→A)-ALP to reach the vacuole or whether A(F→A)-ALP could reach the vacuole by an alternative pathway if trafficking to the PVC is blocked. Vacuolar processing of A(F→A)-ALP was analyzed in a Pep12p temperature-sensitive strain whose function is necessary for all vesicular trafficking into the PVC (Becherer et al., 1996; Gerrard et al., 2000). Wild-type and *pep12-49*^{ts} strains expressing A(F→A)-ALP were shifted to the nonpermissive temperature (36°C) for 10 min, pulsed for 10 min, and chased for the indicated times (Fig. 2 B). In wild-type cells, the processing half-time was ~60 min, whereas processing was essentially blocked in the *pep12-49*^{ts} strain. These results demonstrate that A(F→A)-ALP must traffic to the vacuole via the PVC and, collectively, show that A(F→A)-ALP follows a TGN→EE→PVC pathway before reaching the vacuole.

In contrast to Cps1p, A(F→A)-ALP does not use the GGA pathway to access the endosomal system

The mechanism by which TGN proteins reach the endosomal system appears to involve clathrin because Kex2p and Ste13p/A-ALP are mislocalized to the cell surface in clathrin mutants (Payne and Schekman, 1989; Seeger and Payne, 1992; Ha et al., 2003). Therefore, it is possible that the GGA class of clathrin adaptors may function in this process. The rate of trafficking of A(F→A)-ALP to the PVC/vacuole was previously observed to be unchanged in a *gga1,2Δ* strain compared with wild type (Ha et al., 2001). To address the possibility that A(F→A)-ALP in a *gga1,2Δ* strain was initially mislocalized to the cell surface before being transported to the vacuole, we examined the trafficking kinetics of A(F→A)-ALP in a *gga1,2Δ end3-ts* strain shifted to the nonpermissive temperature by pulse-chase immunoprecipitation. We found no decrease in the trafficking kinetics of A(F→A)-ALP in the *gga1,2Δ end3-ts* strain as compared with *gga1,2Δ* or the wild-type strain (Fig. 2 C). Therefore, the GGAs are dispensable for anterograde trafficking of A(F→A)-ALP into the endosomal system. Moreover, this data suggest that there is a GGA-independent trafficking route that affords access to the PVC via a route that does not include the plasma membrane.

The vacuolar protease Cps1 is initially synthesized as an inactive precursor that is proteolytically processed to yield the mature form upon reaching the vacuole (Cowles et al., 1997). Previously, it was reported that in a *gga1,2*Δ strain, Cps1p transport to the vacuole is delayed (Costaguta et al., 2001). Cps1p contains a ubiquitin moiety that causes it to be sorted into multivesicular body vesicles upon reaching the PVC (Katzmann et al., 2001; Reggiori and Pelham, 2001). As GGA adaptors have been shown to recognize the ubiquitin moiety on cargo proteins at the TGN (Pelham, 2004; Scott et al., 2004), it seems likely that Cps1p enters clathrin/GGA-coated vesicles at the TGN and is directly delivered to the PVC. Using the same experimental regimen as for A(F→A)-ALP (Fig. 2 C) except with different chase times, we also observed a marked delay in Cps1p processing in a *gga1,2*Δ strain (Fig. 3 A), albeit not as dramatic as reported by Costaguta et al. (2001). An even stronger delay was observed in a *gga1,2Δ end3-ts* strain, suggesting that in the absence of GGA function, a pool of Cps1p is mislocalized to the cell surface before being transported to the vacuole via the endocytic pathway. However, even in the *gga1,2Δ end3-ts* strain, Cps1p was slowly processed (61-min half-time), suggesting that in the absence of GGAs, Cps1p was capable of accessing the PVC by an intracellular route, presumably via the EE. Finally, trafficking of Cps1p was blocked by the *pep12-49*^{ts} mutation (Fig. 3 A); thus, like A(F→A)-ALP, Cps1p must transit via the PVC to then be transported to the vacuole. In summary, these results are consistent with a model in which Cps1p uses a GGA-dependent direct TGN to PVC pathway and that A(F→A)-ALP exits the TGN via a GGA-independent pathway leading to the EE.

AP-1 is not required for A(F→A)-ALP to access the GGA-independent pathway to the endosomal system but instead slows its trafficking into the PVC

To address whether the clathrin adaptor AP-1 might function at the TGN for the transport of A(F→A)-ALP to the EE, random

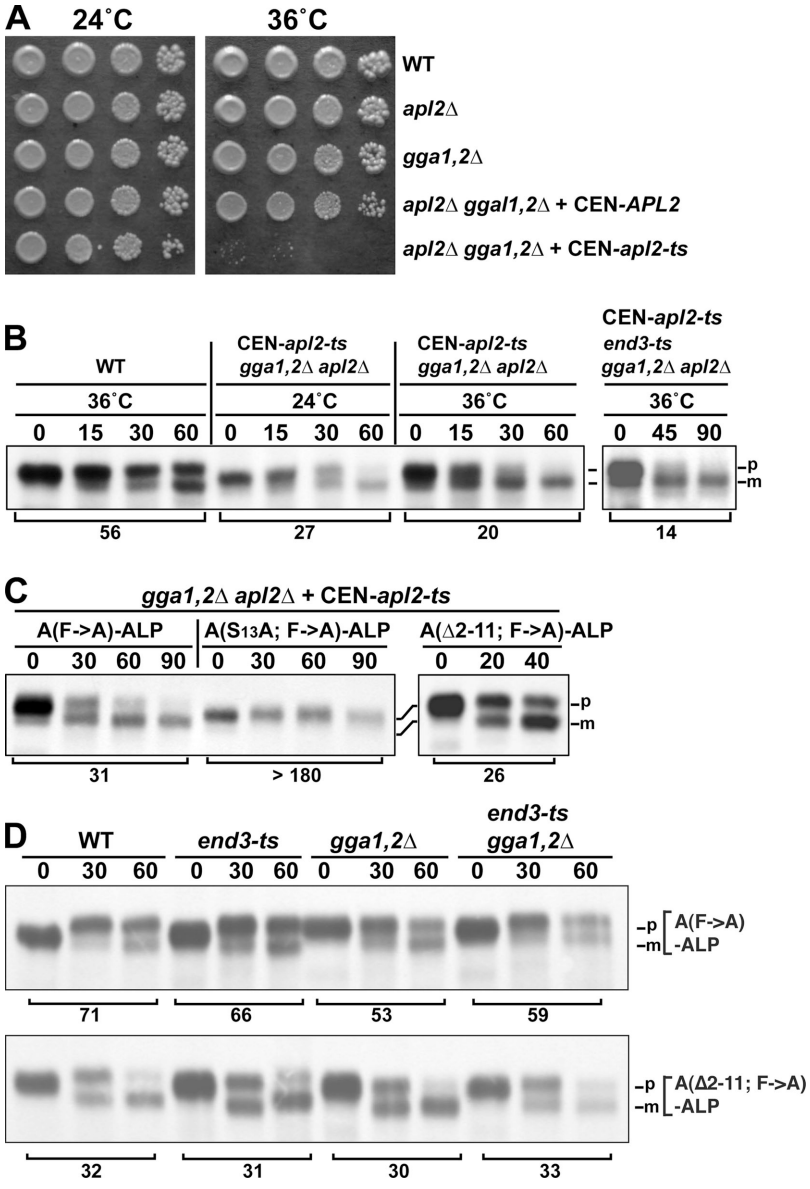

Figure 4. **Both the adaptor complex AP-1 and the Ste13p 2–11 region slow the transport of A(F→A)-ALP through the TGN→EE→PVC pathway rather than being required for anterograde transport.** (A) Strains SHY35 (wild type), UFY2 (*apl2Δ*), SNY165 (*gga1,2Δ*), CFY6-2C/pCF2 (*apl2Δ gga1,2Δ/pCEN-APL2*), and CFY6-2C/pCF6 (*apl2Δ gga1,2Δ/pCEN-apl2-ts*) were analyzed by spotting 10-fold serial dilutions onto YPD media and incubating for 4 d at the indicated temperature. (B) SHY35, CFY6-2C/pCF6, and CFY25-3B/pCF6 (*apl2Δ gga1,2Δ end3-ts/pCEN-apl2-ts*) strains were grown for several doublings at 24°C, shifted to 36°C (or left at 24°C as indicated) for 10 min, pulsed for 10 min, and chased as indicated. (C) Strain CFY6-2C/pCF6 carrying (left to right) plasmids pSN100 (A(F→A)-ALP), pHJ63 (A(S_{13}A; F→A)-ALP), or pSH46 (Δ2–11; F→A)-ALP) was analyzed after shifting from 24 to 36°C as in B. (D) Strains SHY35, SNY94 (*end3-ts*), SNY165, and SNY171-4D carrying pSN100 (top) or pSH46 (bottom) were analyzed after shifting from 24 to 36°C as in B. (B–D) A(F→A)-ALP or its derivatives were immunoprecipitated and analyzed by SDS-PAGE to separate the precursor (p) and mature (m) forms. The half-time of processing of each strain is indicated below each panel.

mutagenesis was used to generate a temperature-sensitive *apl2-ts* mutation. In the presence of the *gga1,2Δ* mutations, the *apl2-ts* allele exhibited near normal growth at 24°C but little or no growth at the nonpermissive temperature of 36°C (Fig. 4 A), which is consistent with the near synthetic lethality previously observed for mutations in these three genes (Costaguta et al., 2001).

We next asked whether the trafficking kinetics of A(F→A)-ALP was altered in this strain lacking both AP-1 and GGA function. In the event that TGN to EE trafficking of A(F→A)-ALP was blocked, including the *gga1,2Δ* mutations would prevent any A(F→A)-ALP from spilling into the GGA-mediated direct TGN to PVC pathway. At 36°C, the *gga1,2Δ apl2-ts* strain exhibited markedly accelerated processing kinetics compared with wild type (20 vs. 56 min; Fig. 4 B). In contrast to the growth characteristics of the *gga1,2Δ apl2-ts* strain (Fig. 4 A), the accelerated processing of A(F→A)-ALP was nearly as pronounced at 24 as at 36°C. Thus, the protein encoded by the *apl2-ts* allele is partially defective for trafficking at the permissive temperature. Furthermore, the accelerated trafficking of A(F→A)-ALP in this strain was also observed in a *gga1,2Δ apl2-ts end3-ts* strain in which both the GGA-mediated direct TGN to PVC and plasma membrane routes are blocked, leaving only the TGN to EE pathway intact. These results imply that AP-1 is not required for A(F→A)-ALP transport to the EE and argue instead that AP-1 functions to slow transport into the PVC, presumably via EE to TGN retrieval.

A(F→A)-ALP is obligated to reach the PVC before being transported to the vacuole (Fig. 2 B). However, we considered the possibility that A(F→A)-ALP might be transported to the vacuole in the *gga1,2Δ apl2-ts* strain by a route not normally used in wild-type cells. One possibility is that in the *gga1,2Δ apl2-ts* strain, regions of the TGN could be transported directly to the vacuole by an autophagic pathway. However, this is unlikely because we did not observe an expected side effect of such an event: a reduction in the amount of protein secretion by the *gga1,2Δ apl2-ts* strain at 36°C compared with wild type (unpublished data). We investigated this further by addressing whether the $S_{13}A$ mutation would block the delivery of A(F→A)-ALP to the PVC/vacuole in the *gga1,2Δ apl2-ts* strain. The $S_{13}A$ mutation blocks the delivery of A(F→A)-ALP to the PVC apparently by preventing its exit from the EE (Johnston et al., 2005). The $S_{13}A$ mutation was found to block the trafficking of A(F→A)-ALP in the *gga1,2Δ apl2-ts* strain (Fig. 4 C), strongly suggesting that A(F→A)-ALP reaches the PVC/vacuole by its normal route in this strain. Furthermore, these results indicate that the $S_{13}A$ trafficking block occurs after the trafficking step that is mediated by AP-1.

The 2–11 region of Ste13p functions in concert with AP-1 in a trafficking step that slows the transport of A(F→A)-ALP into the PVC/vacuole

Like the AP-1 adaptor complex, the role of the 2–11 region of Ste13p is to slow the transport of Ste13p/A-ALP into the PVC (Bryant and Stevens, 1997; Ha et al., 2001; Johnston et al., 2005). The 2–11 region could act as a static retention signal in the TGN or as a signal for EE to TGN retrieval. Another possibility is that it could be necessary for TGN to EE anterograde transport and that deletion of 2–11 might cause accelerated transport into the PVC because A(Δ2–11; F→A)-ALP is forced into alternative pathways (i.e., a direct TGN to PVC pathway or plasma membrane pathway). To address the latter scenario, we assessed the trafficking of A(Δ2–11; F→A)-ALP in a *gga1,2Δ end3-ts* strain in which the alternative pathways were blocked (Fig. 4 D). Deletion of 2–11 caused the acceleration of transport to a similar extent in all four strains examined, including the *gga1,2Δ end3-ts* strain. The absence of a block or delay in transport in the *gga1, 2Δ end3-ts* strain caused by deletion of the 2–11 region argues that this signal plays a role either in EE to TGN retrieval or in static TGN retention.

If the 2–11 region and AP-1 act at the same step, the deletion of 2–11 and the loss of AP-1 function should not cause an additive effect on the acceleration of A(F→A)-ALP trafficking. Consistent with 2–11 and AP-1 acting at the same step, A(Δ2–11; F→A)-ALP was found to exhibit trafficking kinetics in the *gga1,2Δ apl2-ts* strain (26-min half-time; Fig. 4 C) that were similar to A(F→A)-ALP in *gga1,2Δ apl2-ts* (20 min; Fig. 4 B) and A(Δ2–11; F→A)-ALP in *gga1,2Δ* (30 min; Fig. 4 D).

An in vitro binding assay was used to assess whether the heterotetrameric AP-1 complex associates with the Ste13p cytosolic domain. The Ste13p cytosolic domain (residues 1–118) was fused to the NH_2 terminus of GST and the resulting fusion protein (Ste13-GST) purified from *Escherichia coli* onto glutathione-agarose beads. The beads were incubated with protein extracts from a yeast strain containing an epitope-tagged allele (*APM1::HA*) of the μ1 subunit of AP-1 (Yeung et al., 1999). Bead-associated proteins were analyzed by Western blotting for Apm1-HA and Apl2p (Fig. 5). Both AP-1 subunits were found to associate with Ste13-GST but not with GST alone (Fig. 5 A). Interestingly, we observed little or no association of Apm1-HA or Apl2p with Ste13(Δ2–11)-GST, indicating that the interaction is highly dependent on the 2–11 region. Fusions containing only residues 1–20 and 1–12 of Ste13p also bound to AP-1 with similar affinity to that of full-length Ste13-GST. Thus, residues 1–12 are necessary and sufficient for association with Apm1-HA and Apl2p. There appeared to be little, if any, difference in the binding of these AP-1 subunits to the wild-type, $S_{13}A$, and $S_{13}D$ versions of Ste13-GST. Data from a previous study was consistent with the idea that phosphorylated S_{13} might antagonize the 2–11 signal (Johnston et al., 2005); however, this binding data coupled with the observation that the $S_{13}A$ block is downstream of AP-1 would appear to argue against this. Finally, the data suggested that more Apm1-HA than Apl2p was bound to the Ste13-GST beads based on comparison with the amounts of these proteins detected in the input sample. This suggested that Apm1p was binding as a monomer in addition to binding within the context of intact AP-1. Thus, it could be the subunit that Ste13p interacts with directly.

In animal cells, the μ or, less commonly, the β subunit of adaptor complexes recognize cargo proteins (Bonifacino and Traub, 2003; Owen et al., 2004). Given our results suggesting that yeast μ1, or Apm1p, may be the AP-1 subunit that recognizes Ste13p, we asked whether Apm1p expressed in rabbit reticulocyte lysates in the absence of the other yeast AP-1 subunits

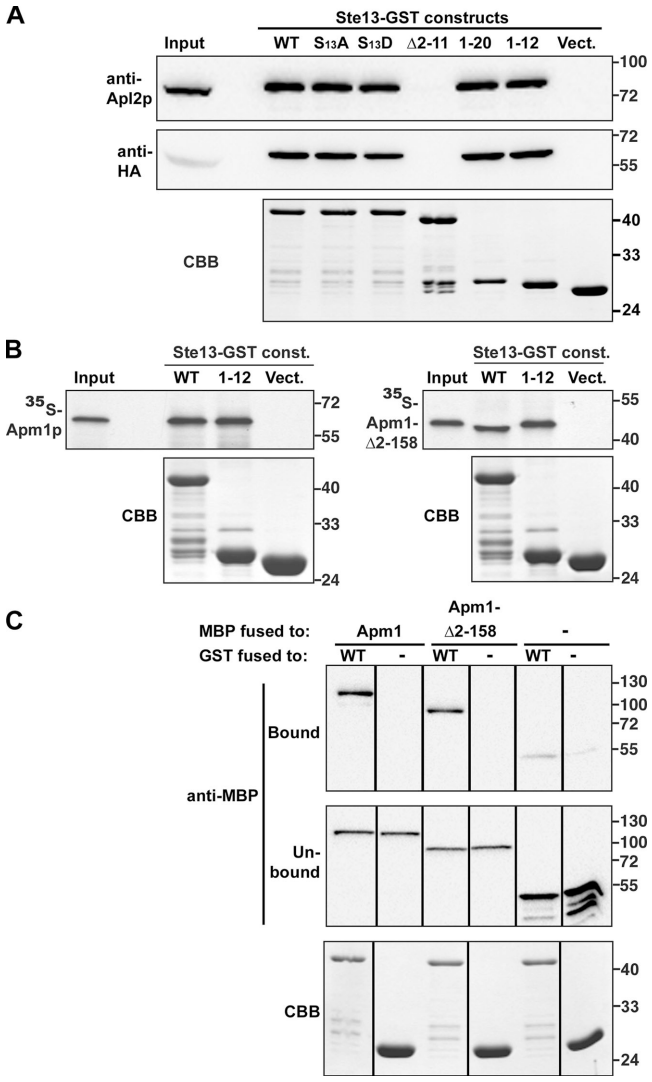

Figure 5. **The clathrin adaptor complex AP-1 directly interacts with amino acids 1–12 of Ste13p.** The following proteins were expressed in *E. coli* and purified onto glutathione-agarose beads: Ste13-GST (WT), Ste13(S_{13}A)-GST (S_{13}A), Ste13(S_{13}D)-GST (S_{13}D), Ste13(1–20)-GST (1-20), Ste13 (1–12)-GST (1-12), and GST (Vect or −). (A) The bead samples were incubated with an SNY190 yeast protein extract followed by washing, elution, and analysis of the eluted proteins by SDS-PAGE. Identical gels were immunoblotted with anti-Apl2p or anti-HA antibodies to detect Apm1-HA as indicated. Yeast extract equivalent to 4% of that incubated with each bead sample was also analyzed (input). The same samples analyzed by Western blotting were also analyzed by staining with Coomassie brilliant blue (CBB) to indicate the relative quantity of each GST fusion. (B) Rabbit reticulocyte lysates programmed with mRNA encoding either Apm1p (left) or an Apm1-Δ2–158 mutant (right) were used to synthesize the corresponding ^{35}S-labeled proteins. Beads prebound to the indicated Ste13-GST constructs were incubated with aliquots of each in vitro translation reaction. After washing, elution, and separation by SDS-PAGE, bead-associated proteins were analyzed by Coomassie staining (bottom) followed by autoradiography (top). The input represents 10% of the translation reaction incubated with each of the bead samples. (C) The following maltose-binding protein (MBP)–derived proteins were expressed in *E. coli*, purified onto amylose resin, and eluted using maltose: MBP-Apm1, MBP–Apm1-Δ2–158, and MBP alone. Beads prebound to Ste13-GST and GST alone were incubated with each MBP-derived protein. Aliquots of proteins not associated with beads (unbound) and proteins that remained associated with beads after washing (bound) were separated by SDS-PAGE and subjected to anti-MBP immunoblotting. Bead-associated samples were also analyzed by Coomassie brilliant blue staining to visualize the GST-derived proteins. For each of the three panels, samples were loaded on the same gel, proteins were detected, and lanes were rearranged for presentation. A total of 60 and 3% of the bound and unbound samples were loaded, respectively, on the indicated gels that were subsequently processed into immunoblots using identical conditions to facilitate comparison. The positions and size (in kilodaltons) of molecular mass standards are indicated.

would bind to Ste13-GST. We found that Ste13-GST and Ste13(1–12)-GST associated with ^{35}S-labeled Apm1p, whereas GST alone did not (Fig. 5 B, left). Mammalian μ subunits contain two independently folding domains: a domain in the NH_2-terminal one third of the protein that mediates association with the β subunit and a domain in the COOH-terminal two thirds of the protein that mediates binding to the YXXΦ class of cargo signals (where Φ stands for an amino acid with a bulky, hydrophobic side chain; Aguilar et al., 1997; Collins et al., 2002). The region of yeast Apm1p corresponding to the mammalian μ cargo-binding domain, Apm1-Δ2–158, associated with Ste13-GST and Ste13(1–12)-GST with a similar efficiency as full-length Apm1p (Fig. 5 B, right). Note that Apm1-Δ2–158 comigrated with Ste13-GST, affecting its mobility relative to the input and Ste13(1–12)-GST pull-down.

As a more stringent test of whether Apm1p/Ste13p binding is direct, we fused full-length Apm1p and Apm1-Δ2–158 to maltose-binding protein (MBP), expressed the fusions in *E. coli*, and purified them using amylose resin affinity chromatography. Ste13-GST immobilized on beads but not GST alone, clearly associating with both MBP-Apm1p and MBP-Apm1-Δ2–158 while it sedimented only background levels of MBP (Fig. 5 C). Collectively, these data show that the 1–12 region of Ste13p associates with the COOH-terminal region of Apm1p directly (i.e., a bridging protein is not required). The broad implication is that AP-1 slows the transport of A(F→A)-ALP into the PVC by associating with the 1–12 region to recruit this cargo protein into clathrin/AP-1 vesicles.

The first 12 amino acids of Ste13p are sufficient to slow the trafficking of Cps1p along the TGN/EE pathway

Cps1p clearly uses a different route than A(F→A)-ALP to reach the PVC because it is delayed by the loss of GGA function (Fig. 3 A). Cps1p does not normally appear to use the EE to PVC route, as a loss of Soi3p function has little or no effect on the rate of trafficking of Cps1p into the PVC (Fig. 3 B).

Residues 1–12 of Ste13p are necessary and sufficient for binding to AP-1 in vitro (Fig. 5), and this region is clearly necessary to slow in vivo trafficking of A(F→A)-ALP into the PVC by acting at the TGN/EE. To test whether the AP-1–binding region of Ste13p is sufficient for in vivo function, we asked whether appending this region to the NH_2-terminal cytosolic domain of Cps1p would slow its trafficking in a *gga1,2Δ* strain. In the *gga1,2Δ* background, trafficking of Cps1p via the direct TGN to PVC pathway is prevented (Fig. 3 A), thus forcing these cargo proteins to access the PVC via the TGN→EE→PVC route or the plasma membrane→EE→PVC route. A construct containing residues 1–23 of Ste13p fused to Cps1p, Ste13-(1–23)-Cps1, was processed rapidly in wild-type cells at a rate similar to wild-type Cps1p, indicating that this fusion accesses

the GGA-mediated pathway to the PVC and does not undergo any aberrant folding or transport delays in the early secretory pathway. However, in *gga1,2Δ* cells, Ste13(1–23)-Cps1 is processed significantly more slowly (54 ± 5-min half-time) than Cps1p in the *gga1,2Δ* strain (34 ± 2 min). This difference is comparable with the difference between A(F→A)-ALP (53 min) and A(Δ2–11; F→A)-ALP (30 min) observed in *gga1,2Δ* cells (Fig. 4 D). Thus, this Ste13p NH_2-terminal region slows the trafficking of Ste13-Cps1 most likely by mediating its retrieval from the EE. Importantly, a $S_{13}A$ mutation in the Ste13(1–23)-Cps1 context markedly slowed trafficking in the *gga1,2Δ* strain (98 ± 11 min). Because the $S_{13}A$ block appears to occur at the level of the EE (Johnston et al., 2005), this result indicates that the Ste13-Cps1 fusions do indeed traffic to the PVC via the EE as expected. A similar reduction in trafficking was observed when just residues 1–12 of Ste13p were fused to Cps1p (48 ± 3 min). Collectively, the data indicate that the first 12 residues of Ste13p are both necessary and sufficient to slow trafficking into the PVC.

Discussion

A major goal of this study was to address the respective roles of the clathrin adaptors AP-1 and GGAs in the trafficking of A(F→A)-ALP, a model TGN protein based on Ste13p. Our results suggest that AP-1 functions in retrograde EE to TGN transport of A(F→A)-ALP. In addition, we demonstrate a physical interaction between a Ste13p cytosolic domain region and AP-1 and describe, for the first time, a cargo-sorting signal recognized by the yeast AP-1 adaptor.

A(F→A)-ALP is delivered to the PVC via the EE

Three independent experiments suggested that the pathway by which A(F→A)-ALP reaches the PVC involves EEs. First, GFP-tagged A-ALP was found to partially colocalize with the endocytic tracer dye FM4-64 at a time point when it was primarily localized to EEs. Second, the loss of function of Soi3p necessary for efficient EE to PVC trafficking markedly delayed the trafficking of A(F→A)-ALP to the PVC. Finally, the loss of function of GGA clathrin adaptors, which appear to function in the direct TGN to PVC pathway (see Introduction), did not delay the trafficking of A(F→A)-ALP to the PVC or cause it to be mislocalized to the plasma membrane. This was in contrast to Cps1p that was delayed in strains lacking GGA function (Fig. 3; Costaguta et al., 2001). In *gga1,2Δ* cells, Cps1p eventually reached the PVC/vacuole in part via the plasma membrane.

Whereas our data argues that little, if any, A(F→A)-ALP traffics through the direct TGN to PVC pathway, the situation may be a bit different for Kex2p. In contrast to A(F→A)-ALP, Kex2p trafficking into the PVC was delayed somewhat because of a loss of GGA function (Costaguta et al., 2001). In addition, Kex2p is transported into the PVC significantly more rapidly than A-ALP as judged by processing/turnover in a *vps27* class E mutant (Ha et al., 2001; Sipos et al., 2004). This is consistent with the partitioning of Kex2p between a direct TGN to PVC pathway and the TGN→EE→PVC route.

In cells lacking both GGA and End3p function, Cps1p was able to reach the PVC, albeit slowly, suggesting that it is able to access the TGN to EE pathway. It seems unlikely that Cps1p would contain a cryptic targeting signal for transport to the EE. Thus, it is possible that that TGN to EE trafficking can occur by default rather than in a strictly signal-mediated fashion. According to the cisternal maturation view of Golgi trafficking, the EE may be a mature post-TGN compartment depleted of secretory as well as PVC-bound cargo that has fused with endocytic vesicles (Pelham, 1998). This would explain why Cps1p that is unable to undergo TGN to PVC transport would be swept along to the EE and, to a limited degree, the plasma membrane.

Role of AP-1 in cargo sorting

One of our major objectives was to address whether AP-1 is needed for anterograde TGN to EE trafficking of A(F→A)-ALP. It was shown previously that the loss of function of the AP-1 β-subunit Apl2p did not delay the trafficking of A(F→A)-ALP to the PVC and, in fact, accelerated it slightly (Ha et al., 2003). Because it was possible that in *apl2* mutants A(F→A)-ALP could reach the PVC by alternative routes, we assessed trafficking in *gga1,2Δ apl2-ts* and *gga1,2Δ apl2-ts end3-ts* strains. In both cases, trafficking was markedly accelerated relative to a wild-type strain. A(F→A)-ALP appeared to reach the PVC by the normal TGN→EE→PVC route because a $S_{13}A$ mutation previously shown to prevent EE to PVC transport of A(F→A)-ALP (Johnston et al., 2005) was shown to also block trafficking in the *gga1,2Δ apl2-ts* strain. Furthermore, secretory pathway function of the *gga1,2Δ apl2-ts* strain appeared normal, ruling out any large-scale autophagic transport of TGN membranes to the vacuole that might have explained the accelerated transport.

Collectively, our results indicate that AP-1 is not required for anterograde TGN to EE transport of A(F→A)-ALP. However, we cannot entirely exclude the possibility that AP-1 is involved in anterograde trafficking and that in the *gga1,2Δ apl2-ts* strain, another protein complex redundant with AP-1 was able to fill in for its absence. Indeed, the role of AP-1 in animal cells has been controversial, with both evidence supporting a role for AP-1 in anterograde trafficking out of the TGN to endosomes (Huang et al., 2001; Puertollano et al., 2003) and other evidence implicating AP-1 in the retrograde transport of cargo from endosomes and post-Golgi secretory granules to the TGN (Klumperman et al., 1998; Meyer et al., 2000). However, a role for yeast AP-1 in exit from the TGN would not explain why the trafficking of A(F→A)-ALP is accelerated. Rather, the results seem to point to a role for AP-1 in slowing the transport of A(F→A)-ALP through the TGN→EE→PVC pathway. In principle, this could occur by clathrin/AP-1 mediating either vesicular retrieval from the EE back to the TGN (see Fig. 7 A) or mediating static retention in the TGN (see Fig. 7 B). We tend to favor the former model because it fits better with the known role of clathrin/AP-1 as a vesicle coat. In addition, the loss of AP-1 function caused Chs3p to be mislocalized to the cell surface under conditions in which it would normally be localized to EEs. As Chs3p appears to maintain its EE localization by cycling

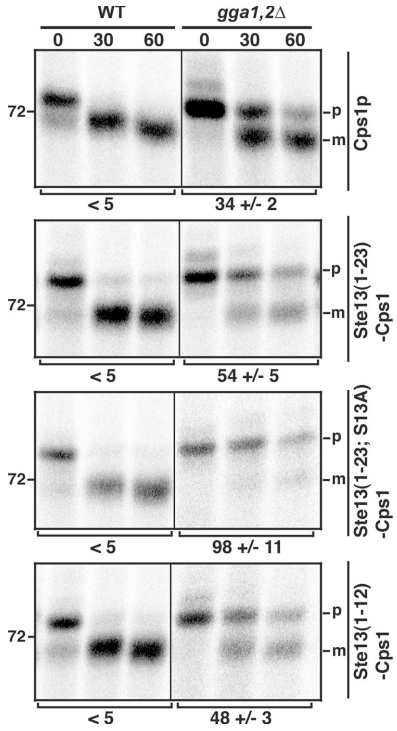

Figure 6. **Residues 1–12 of Ste13p are sufficient to slow the trafficking of Cps1p into the PVC/vacuole.** Yeast strains CFY30 (*cps1Δ*) and CFY32 (*cps1Δ gga1,2Δ*) carrying plasmids expressing Cps1p, Ste13(1–23)-Cps1, Ste13(1–23; S_{13}A)-Cps1, and Ste13(1–12)-Cps1 were subjected to pulse-chase analysis at 30°C and immunoprecipitation as described in Fig. 3. The half-time of processing is indicated below each panel. The *gga1,2Δ* half-times are provided as the average and SD of two independent datasets. The positions and size (in kilodaltons) of molecular mass standards are indicated. p, precursor form; m, mature form.

to and from the TGN, the results were interpreted to mean that AP-1 plays a role in the EE to TGN retrieval of Chs3p (Valdivia et al., 2002). The Snx4–Snx41–Snx42 complex has also been implicated in EE to TGN retrieval of the v-SNARE Snc1p (Hettema et al., 2003). Similarly, the F-box protein Rcy1p was implicated in EE to TGN trafficking of both Snc1p and Kex2p (Chen et al., 2005). However, neither the loss of function of the Snx4–Snx41–Snx42 complex nor Rcy1p appear to affect the trafficking of A(F→A)-ALP (unpublished data). In summary, we propose that the slow rate of A(F→A)-ALP transport into the PVC is caused by repeated rounds of EE/TGN cycling brought about by clathrin/AP-1–mediated retrieval from the EE. A loss of AP-1 and possibly GGA function would then cause A(F→A)-ALP to access the EE to PVC pathway, accounting for the accelerated transport into the PVC.

Although there is good evidence that the GGA adaptors play an important role in the direct TGN to PVC pathway, it is also possible that the GGAs may function with AP-1 in trafficking between the TGN and EE. This proposal is based on the observation that the acceleration of A(F→A)-ALP trafficking into the PVC is very weak in *apl2* single mutants (Ha et al., 2003). Furthermore, we often see a slight acceleration in trafficking in *gga1,2Δ* mutants reminiscent of that observed in *apl2* mutants (Fig. 2). Thus, one possibility is that AP-1 and the GGAs may have an overlapping function for the EE to TGN retrieval step. It is relevant that both AP-1 and GGAs are present on the same vesicles and tubules budding from the mammalian TGN (Puertollano et al., 2003) and that the interaction of AP-1 with GGAs has been observed in both yeast and animal cells (Costaguta et al., 2001; Doray et al., 2002; Bai et al., 2004). Furthermore, mammalian GGAs mediate EE to TGN recycling of memapsin 2 (BACE; He et al., 2005). It is possible that redundancy between AP-1 and the GGAs exists such that the function of both adaptors needs to be lost to observe a strong defect in EE to TGN retrieval. On the other hand, we have detected little, if any, Gga2p binding to the cytosolic domain of Ste13p in pull-down assays (unpublished data), suggesting that the GGAs do not function in Ste13p cargo recognition.

A novel signal in Ste13p for interaction with AP-1

Residues 2–11 of Ste13p/A-ALP are necessary for its effective retention within the TGN/EE system (Bryant and Stevens, 1997). We observed that even with both the direct TGN to PVC and plasma membrane pathways blocked in a *gga1,2Δ end3-ts* strain, the deletion of residues 2–11 from A(F→A)-ALP accelerated its trafficking into the PVC. Furthermore, when Cps1p was forced to traffic into the PVC via the EE in a *gga1,2Δ* strain, its rate of transport to the vacuole significantly decreased as a result of fusing residues 1–12 of Ste13p/A-ALP to the NH_2 terminus of its cytosolic domain (Fig. 6). These results imply that this NH_2-terminal region contains a signal needed to slow trafficking through the EE and suggest that this signal may mediate EE to TGN retrieval. In support of this, we observed an interaction between the Ste13p cytosolic domain and AP-1 subunits in vitro that was dependent on residues 2–11. Remarkably, Apm1-HA and Apl2p associated with a GST fused to residues 1–12 of Ste13p with an efficiency similar to that of the entire Ste13p cytosolic domain fused to GST. This data, along with the observation that 1–12 is sufficient to slow Cps1p trafficking into the PVC in a *gga1,2Δ* strain, suggests that residues 1–12 make most, if not all, of the specific contacts with AP-1. However, sequences COOH-terminal to this region might be required for optimal interaction by supplying additional contacts with AP-1 and/or for properly presenting the 1–12 region to AP-1.

This study provides the first glimpse into signal-mediated sorting by yeast AP-1. Previously described signals mediating AP-1–cargo interactions in animal cells include the YXXΦ signal that binds to the μ1 subunit and (D or E)XXXL(L or I), which binds either to the β1 or μl subunits (Bonifacino and Traub, 2003). The Ste13p motif ($MSASTHSHKRKN_{12}$) is a striking departure from these well-characterized signals in animal cells. One obvious feature is a cluster of positively charged residues. The residues within this region that are critical for AP-1 binding are not yet known; however, the S2, S4, and S7 residues have been mutated to alanine without any detectable acceleration in the trafficking of A(F→A)-ALP into the PVC (Johnston et al., 2005). Our data indicate that a COOH-terminal region of yeast μ1 is sufficient to bind the 12-residue Ste13p motif (Fig. 5) and, thus, must contain most or all of the critical residues that contact the 12-residue signal.

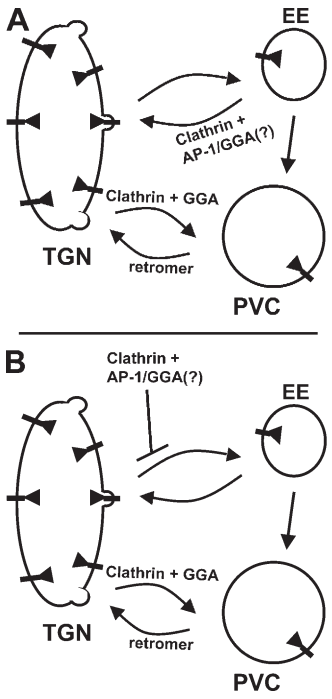

Figure 7. **Models for the role of clathrin/AP-1 in the sorting of A(F→A)-ALP.** (A) A(F→A)-ALP undergoes repeated rounds of cycling between the TGN and EE that involve sorting into clathrin/AP-1–coated vesicles at the EE. (B) Clathrin/AP-1 mediates the static retention of A(F→A)-ALP at the TGN. In both models, sorting is mediated by the interaction of AP-1 with residues 1–12 of A(F→A)-ALP. The GGA clathrin adaptors may participate with AP-1 in sorting A(F→A)-ALP.

The relationship of the AP-1–interacting domain at residues 1–12 to the S_{13} phosphorylation site is intriguing. Deletion of residues 2–11 negated the effect of S_{13}A and S_{13}D mutations meant to mimic the unphosphorylated and phosphorylated states, respectively (Johnston et al., 2005). These data suggested that the role of phosphorylated S_{13} may be to regulate (antagonize) the 2–11 region. In this view, a S_{13}A mutation would make the AP-1–interacting domain (and, thus, EE to TGN retrieval) much more effective than normal. However, data presented in this study appear to refute this idea. First, a S_{13}A mutation thought to prevent EE to PVC transport caused a block in the processing of A(F→A)-ALP in the *gga1,2Δ apl2-ts* strain (Fig. 4 C). If S_{13} were simply regulating the AP-1–interacting domain at residues 1–12, there should not have been a delay in trafficking to the PVC as a result of the S_{13}A mutation when AP-1 function was lost. Second, in vitro binding of AP-1 with residues 1–12 is not significantly affected by the S_{13}A and S_{13}D mutations (Fig. 5), although modest differences in binding affinities might not be revealed by in vitro pull-down assays. Nevertheless, these results argue that the signal regulated by the phosphorylation of S_{13}, which, in turn, regulates EE to PVC trafficking, is distinct from the 1–12 signal that is recognized by AP-1.

What, then, is the role of the S_{13} signal? The phosphorylated S_{13} signal does not seem to be required for EE to PVC transport. For example, Ste13(1–23)-Cps1p, which clearly contains at least some aspects of the signal based on the results of a S_{13}A mutation within this protein, has essentially the same kinetics of transport in a *gga1,2Δ* strain as Ste13(1–12)-Cps1, which lacks the signal (Fig. 6). In addition, A(Δ2–11)-ALP, which seems to have lost critical elements of the signal based on the fact that the S_{13}A mutation has no effect in this protein (Johnston et al., 2005), is transported into the PVC more rapidly than A-ALP. The A(Δ2–11; F→A)-ALP protein appears to use the TGN→EE→PVC pathway (Fig. 7). Thus, the data do not support the view that phosphorylated S_{13} is needed for EE to PVC transport. Rather, the data support a model in which unphosphorylated S_{13} acts as a signal to somehow prevent EE to PVC transport, apparently by retaining Ste13p in the EE. Future work will be directed toward a more precise structural and functional definition of the AP-1 and S_{13} signals.

Materials and methods

General methods and antibodies

The production of yeast media, the genetic manipulation of yeast strains, and all general molecular biology methods were performed as described previously (Ausubel et al., 2002) or as otherwise noted. Rabbit polyclonal antibodies against ALP have been previously described (Nothwehr et al., 1996; Spelbrink and Nothwehr, 1999). Rabbit anti-HA epitope and rabbit anti-MBP antibodies were obtained from Covance and New England Biolabs, Inc., respectively. Rabbit polyclonal antibodies against Cps1p were raised against a fusion protein consisting of GST fused to residues 46–577 of Cps1p, whereas rabbit anti-Apl2p antibodies were gifts from G. Payne (University of California, Los Angeles, Los Angeles, CA).

DNA manipulations and yeast strains

Plasmids pSN55, pSN100, and pHJ63 have been previously described (Nothwehr et al., 1993; Johnston et al., 2005). The GFP–A-ALP construct pCF17 is p416-CYC (Mumberg et al., 1995) containing PCR-derived sgGFP (Qbiogene) followed by a $(GlyAla)_3$ linker and the coding region of *STE13-PHO8* (Nothwehr et al., 1993) starting with codon 2. pCF4, CEN-*CPS1* was constructed by inserting a 4.97-kbp XbaI–XhoI fragment excised from pDP83-CPS1 (Spormann et al., 1991) into the same sites in pRS316. Plasmid pCF2 was constructed by inserting a PCR fragment containing the full-length *APL2* ORF into the EcoRI–SalI sites of pRS316. pSH46 was made by swapping a 0.5-kbp EagI–BglII fragment containing the 5′ region of *STE13* with the Δ2–11, F_{85}A, and F_{87}A mutations for the corresponding fragment in pSN55. The Ste13-GST fusion constructs were made by introducing PCR or oligonucleotide duplex-derived inserts into the vector pETGEXCT (Sharrocks, 1994). Fusion of the Apm1p and Apm1-Δ2–158 coding sequences to the MBP sequence was performed by inserting PCR-derived inserts into the vector pMAL-c2 (New England Biolabs, Inc.). Ste13-Cps1 fusion protein constructs consisted of the PCR-derived *STE13* promoter and relevant coding regions fused to the 5′ end of the *CPS1* coding region and 3′ untranslated regions cloned into pRS316 (Sikorski and Hieter, 1989). The fusion junction of the Ste13(1–23)-Cps1 and Ste13-(1–12)-Cps1 fusions were …$KSSN_{23}$GSMIA… and …RKN_{12}GAIAL…, respectively, with the numbered residue representing the last Ste13p residue and the underlined residues indicating the Cps1p sequence.

To construct the *apl2-ts* allele, the *APL2* ORF was amplified via PCR using an error-prone polymerase, Genemorph (Stratagene). The resulting population of PCR products was introduced into pRS313 via homologous recombination in yeast CFY6-2C/pCF2. His+ yeast transformants were then plated onto 5-FOA to lose pCF2 followed by screening for a lack of growth at 37°C and normal growth at 23°C. Finally, the mutagenized Apl2p-expressing plasmids rescued from temperature-sensitive yeast strains were retransformed back into CFY6-2C/pCF2 to test whether the growth phenotype was linked to the plasmid.

All yeast strains are described in Table I. SNY171-4D is a spore derived from a diploid made by crossing SNY165 and SNY94. SHY64 was constructed by mating type-switching UFY2. CFY6-2C is a spore derived from a diploid made by crossing SNY165/pCF2 and SHY64. CFY25-3B is a spore derived from a diploid made by crossing CFY6-2C/pCF6 with SNY94. CFY30, CFY31, CFY32, and CFY33 were all constructed using PCR-mediated gene replacement (Wach et al., 1994) of CPS1 with the NatR marker gene. The *APM1::HA-URA3* allele was integrated at the *APM1* locus using plasmid pAPM1-HA::URA3 (a gift from G. Payne), resulting in strain SNY190.

Table I. ***Saccharomyces cerevisiae* strains used in this study**

Strain/plasmid	Description	Origin or reference
SNY36-9A	*MATa leu2-3,112 ura3-52 his3-Δ200 trp1-Δ901 suc2-Δ9 pho8Δ::ADE2*	Nothwehr et al., 1995
SNY94	SNY36-9A *end3-ts*	Spelbrink and Nothwehr, 1999
SNY156	SNY36-9A *pep12-49*^{ts}	Bruinsma et al., 2004
CFY31	SNY156 *cps1Δ::NatR*	This study
LSY2	SNY36-9A *pep4Δ::TRP1*	Spelbrink and Nothwehr, 1999
CFY37	SNY36-9A *vps8Δ::KanR*	This study
CFY38	SNY36-9A *soi3Δ::KanR*	This study
SHY35	SNY36-9A mating type switched	Ha et al., 2001
CFY30	SHY35 *cps1Δ::NatR*	This study
UFY2	SHY35 *apl2::KanR*	Ha et al., 2003
SHY64	UFY2 mating type switched	This study
CFY6-2C/pCF2	*MATα leu2-3,112 ura3-52 his3-Δ200 trp1-Δ901 suc2-Δ9 pho8Δ::ADE2 apl2Δ::KanR gga1Δ::TRP1 gga2Δ::KanR* + pCF2	This study
CFY6-2C/pCF6	*MATα leu2-3,112 ura3-52 his3-Δ200 trp1-Δ901 suc2-Δ9 pho8Δ::ADE2 apl2Δ::KanR gga1Δ::TRP1 gga2Δ::KanR* + pCF6	This study
CFY25-3B/pCF6	*MATα leu2-3,112 ura3-52 his3-Δ200 trp1-Δ901 suc2-Δ9 apl2Δ::KanR gga1Δ::TRP1 gga2Δ::KanR end3-ts (pho8-ΔX or pho8Δ::ADE2)* +pCF6	This study
SNY165	*MATα leu2-3,112 ura3-52 his3-200 trp1-90 lys2-801 suc2-9 pho8-X gga1Δ::TRP1 gga2Δ::KanR*	Ha et al., 2003
CFY32	SNY165 *cps1Δ::NatR*	This study
SNY171-4D	*MATα leu2-3,112 ura3-52 his3-200 trp1-90 lys2-801 suc2-9* (*pho8-ΔX* or *pho8Δ::ADE2*) *gga1Δ::TRP1 gga2Δ::KanR* end3-ts	This study
CFY33	SNY171-4D *cps1Δ::NatR*	This study
TVY614	*MATα ura3-52 leu2-3,112 his3-Δ200 trp1-Δ901 lys2-801 suc2-Δ9 prb1Δ::HISG prc1Δ::HIS3*	T. Vida[a]
SNY190	TVY614 *pho8-ΔX APM1::HA-URA3*	This study

[a]The University of Texas Medical School at Houston, Houston, TX.

Radioactive labeling, immunoprecipitation, and Western blot analysis

The procedure for immunoprecipitation of wild-type and mutant A-ALP from [^{35}S]methionine/cysteine-labeled cells and Western blotting has been previously described (Nothwehr et al., 1993; Ha et al., 2003; Johnston et al., 2005). Radioactively labeled proteins were quantified from gels using a phosphorimager system (FLA-2000; Fuji Film). For calculation of the half-time of A-ALP and Ste13-Cps1 processing, the log of the percentage of unprocessed precursor at each time point was plotted as a function of time, and the plots were analyzed by linear regression analysis. Immunoprecipitated Cps1p and derivatives were treated by endoglycosidase H before SDS-PAGE analysis according to a published protocol (Orlean et al., 1991). The precursor and mature forms of the immunoprecipitated A(F→A)-ALP, A(Δ2–11, F→A)-ALP, and Cps1p shown in Figs. 2–4 migrated on SDS-PAGE in a manner consistent with their predicted sizes.

Binding assays

The various GST fusion proteins were expressed in *E. coli* BL21(DE3) (Novagen) and were affinity purified onto glutathione-agarose beads (Sigma-Aldrich). MBP, MBP-Apm1, and MBP-Apm1-Δ2–158 were expressed in *E. coli* BL21, affinity purified onto amylose resin (New England Biolabs, Inc.), and were eluted with buffer containing 10 mM maltose.

The binding of Ste13-GST and its various mutant derivatives with AP-1 was assayed as previously described (Ghosh and Kornfeld, 2004). In brief, 1,000 OD_{600} units of SNY190 cells were spheroplasted, pelleted at 450 *g*, and washed once in 40 ml of ice-cold 1.2 M sorbitol. Spheroplasts were resuspended in 10 ml of buffer C (25 mM Hepes-KOH, pH 7.2, 125 mM potassium acetate, 2.5 mM magnesium acetate, 1 mM DTT, 0.1% Triton X-100, 0.5 mM PMSF, 1 μg/ml leupeptin, and 1 μg/ml pepstatin A), Dounce homogenized, and centrifuged at 20,000 *g* for 15 min. The supernatant was then transferred to a fresh tube and was incubated with a 0.75-ml bed volume of glutathione-agarose beads for 1 h at 4°C. The beads were pelleted at 750 *g*, a 100-μl input sample was saved for gel analysis, the remaining supernatant was split into seven equal portions, and each portion was incubated with a 100-μl bed volume of glutathione-agarose coated with Ste13-GST (or derivatives) for 3 h at 4°C. Samples were washed five times in buffer C followed by elution with SDS-PAGE sample buffer and heating at 100°C for 5 min. Eluted proteins were analyzed by SDS-PAGE and immunoblotting.

Pull-down of in vitro translated wild-type and mutant Apm1p was performed by first translating Apm1p and Apm1-Δ2–158 in rabbit reticulocyte lysates (Ambion) in the presence of [^{35}S]methionine according to the manufacturer's instructions. Glutathione-agarose prebound to GST and GST fusions were incubated with aliquots of each translation reaction diluted with buffer C for 90 min at 4°C in a total volume of 400 μl. The beads were then washed five times with buffer C and were eluted with SDS-PAGE sample buffer at 100°C. Eluted proteins were analyzed by SDS-PAGE and autoradiography.

To test for direct Apm1p-Ste13p interaction, binding assays were performed as described above for the in vitro translated Apm1p except that purified MBP-Apm1, MBP–Apm1-Δ2–158, and MBP alone were incubated with the bead samples.

Microscopy

Cells harvested from log-phase cultures were incubated for 30 min in YPD media containing 0.02 mg/ml FM4-64 (Invitrogen). They were then washed twice with YP media (lacking glucose) and once with SD-ura media before being resuspended in SD-ura media. Up to this point, all steps were performed at 0–4°C. The cells were then incubated at 30°C for 2 or 8 min, immediately placed on ice, and metabolic activity was stopped with 10 mM NaN_3 and 10 mM NaF. The cells were mounted on 2% agarose pads on microscope slides containing 10 mM NaN_3 and 10 mM NaF. The cells were immediately imaged at room temperature for FM4-64 and GFP staining using an epifluorescence microscope (DM5000B) equipped with a 100× NA 1.4 HCX plan-Apo lens, digital camera (DFC350X), and FW4000 software (all from Leica). Images were overlaid using the FW4000 software, adjusted slightly for brightness and contrast, and formatted using Adobe Photoshop 7.0.

We acknowledge Holly Johnston and Seon-Ah Ha for their involvement at various stages of this work and Per Stromhaug for critical reading of the manuscript and advice. Gregory Payne supplied constructs and antibodies.

This work was supported by grants from the National Institutes of Health (R01GM053449 to S.F. Nothwehr and predoctoral training grant 5T32GM008396 to C. Foote).

Submitted: 28 October 2005
Accepted: 18 April 2006

References

Abazeed, M.E., J.M. Blanchette, and R.S. Fuller. 2005. Cell-free transport from the trans-Golgi network to late endosome requires factors involved in formation and consumption of clathrin-coated vesicles. *J. Biol. Chem.* 280:4442–4450.

Aguilar, R.C., H. Ohno, K.W. Roche, and J.S. Bonifacino. 1997. Functional domain mapping of the clathrin-associated adaptor medium chains mu-1 and mu-2. *J. Biol. Chem.* 272:27160–27166.

Ausubel, F.M., R. Brent, R.E. Kingston, D.D. Moore, J.G. Seidman, K. Struhl, and J.A. Smith. 2002. Short Protocols in Molecular Biology: a Compendium of Methods from Current Protocols in Molecular Biology. 5th ed. John Wiley & Sons Inc., New York.

Bai, H., B. Doray, and S. Kornfeld. 2004. GGA1 interacts with the adaptor protein AP-1 through a WNSF sequence in its hinge region. *J. Biol. Chem.* 279:17411–17417.

Becherer, K.A., S.E. Rieder, S.D. Emr, and E.W. Jones. 1996. Novel syntaxin homologue, Pep12p, required for the sorting of lumenal hydrolases to the lysosome-like vacuole in yeast. *Mol. Biol. Cell*. 7:579–594.

Black, M.W., and H.R. Pelham. 2000. A selective transport route from Golgi to late endosomes that requires the yeast GGA proteins. *J. Cell Biol.* 151:587–600.

Bonifacino, J.S., and L.M. Traub. 2003. Signals for sorting of transmembrane proteins to endosomes and lysosomes. *Annu. Rev. Biochem.* 72:395–447.

Brickner, J.H., and R.S. Fuller. 1997. *SOI1* encodes a novel, conserved protein that promotes TGN-endosomal cycling of Kex2p and other membrane proteins by modulating the function of two TGN localization signals. *J. Cell Biol.* 139:23–26.

Bruinsma, P., R.G. Spelbrink, and S.F. Nothwehr. 2004. Retrograde transport of the mannosyltransferase Och1p to the early Golgi requires a component of the COG transport complex. *J. Biol. Chem.* 279:39814–39823.

Bryant, N.J., and T.H. Stevens. 1997. Two separate signals act independently to localize a yeast late Golgi membrane protein through a combination of retrieval and retention. *J. Cell Biol.* 136:287–297.

Chen, S.H., S. Chen, A.A. Tokarev, F. Liu, G. Jedd, and N. Segev. 2005. Ypt31/32 GTPases and their novel F-box effector protein Rcy1 regulate protein recycling. *Mol. Biol. Cell*. 16:178–192.

Collins, B.M., A.J. McCoy, H.M. Kent, P.R. Evans, and D.J. Owen. 2002. Molecular architecture and functional model of the endocytic AP2 complex. *Cell*. 109:523–535.

Cooper, A.A., and T.H. Stevens. 1996. Vps10p cycles between the late-Golgi and prevacuolar compartments in its function as the sorting receptor for multiple yeast vacuolar hydrolases. *J. Cell Biol.* 133:529–541.

Costaguta, G., C.J. Stefan, E.S. Bensen, S.D. Emr, and G.S. Payne. 2001. Yeast Gga coat proteins function with clathrin in Golgi to endosome transport. *Mol. Biol. Cell*. 12:1885–1896.

Cowles, C.R., W.B. Snyder, C.G. Burd, and S.D. Emr. 1997. Novel Golgi to vacuole delivery pathway in yeast - identification of a sorting determinant and required transport component. *EMBO J.* 16:2769–2782.

Dell'Angelica, E.C., R. Puertollano, C. Mullins, R.C. Aguilar, J.D. Vargas, L.M. Hartnell, and J.S. Bonifacino. 2000. GGAs: A family of ADP ribosylation factor-binding proteins related to adaptors and associated with the Golgi complex. *J. Cell Biol.* 149:81–93.

Deloche, O., B.G. Yeung, G.S. Payne, and R. Schekman. 2001. Vps10p transport from the *trans*-Golgi network to the endosome is mediated by clathrin-coated vesicles. *Mol. Biol. Cell*. 12:475–485.

Doray, B., P. Ghosh, J. Griffith, H.J. Geuze, and S. Kornfeld. 2002. Cooperation of GGAs and AP-1 in packaging MPRs at the trans-Golgi network. *Science*. 297:1700–1703.

Gerrard, S.R., B.P. Levi, and T.H. Stevens. 2000. Pep12p is a multifunctional yeast syntaxin that controls entry of biosynthetic, endocytic, and retrograde traffic into the prevacuolar compartment. *Traffic*. 1:259–269.

Ghosh, P., and S. Kornfeld. 2004. The cytoplasmic tail of the cation-independent mannose 6-phosphate receptor contains four binding sites for AP-1. *Arch. Biochem. Biophys.* 426:225–230.

Ha, S.H., J.T. Bunch, H. Hama, D.B. DeWald, and S.F. Nothwehr. 2001. A novel mechanism for localizing membrane proteins to the yeast trans-Golgi network requires function of a synaptojanin-like protein. *Mol. Biol. Cell*. 12:3175–3190.

Ha, S.A., J. Torabinejad, D.B. DeWald, M.R. Wenk, L. Lucast, P. De Camilli, R.A. Newitt, R. Aebersold, and S.F. Nothwehr. 2003. The synaptojanin-like protein Inp53/Sjl3 functions with clathrin in a yeast TGN-to-endosome pathway distinct from the GGA protein-dependent pathway. *Mol. Biol. Cell*. 14:1319–1333.

He, X., F. Li, W.P. Chang, and J. Tang. 2005. GGA proteins mediate the recycling pathway of memapsin 2 (BACE). *J. Biol. Chem.* 280:11696–11703.

Hettema, E.H., M.J. Lewis, M.W. Black, and H.R. Pelham. 2003. Retromer and the sorting nexins Snx4/41/42 mediate distinct retrieval pathways from yeast endosomes. *EMBO J.* 22:548–557.

Hirst, J., W.W.Y. Lui, N.A. Bright, N. Totty, M.N.J. Seaman, and M.S. Robinson. 2000. A family of proteins with γ-adaptin and VHS domains that facilitate trafficking between the trans-Golgi network and the vacuole/lysosome. *J. Cell Biol.* 149:67–79.

Holthuis, J.C.M., B.J. Nichols, S. Dhruvakumar, and H.R.B. Pelham. 1998. Two syntaxin homologues in the TGN/endosomal system of yeast. *EMBO J.* 17:113–126.

Huang, F., A. Nesterov, R.E. Carter, and A. Sorkin. 2001. Trafficking of yellow-fluorescent-protein-tagged μ1 subunit of clathrin adaptor AP-1 complex in living cells. *Traffic*. 2:345–357.

Johnston, H.D., C. Foote, A. Santeford, and S.F. Nothwehr. 2005. Golgi-to-late endosome trafficking of the yeast pheromone processing enzyme Ste13p is regulated by a phosphorylation site in its cytosolic domain. *Mol. Biol. Cell*. 16:1456–1468.

Katzmann, D.J., M. Babst, and S.D. Emr. 2001. Ubiquitin-dependent sorting into the multivesicular body pathway requires the function of a conserved endosomal protein sorting complex, ESCRT-I. *Cell*. 106:145–155.

Klumperman, J., R. Kuliawat, J.M. Griffith, H.J. Geuze, and P. Arvan. 1998. Mannose 6-phosphate receptors are sorted from immature secretory granules via adaptor protein AP-1, clathrin, and syntaxin 6-positive vesicles. *J. Cell Biol.* 141:359–371.

Lewis, M.J., B.J. Nichols, C. Prescianotto-Baschong, H. Riezman, and H.R.B. Pelham. 2000. Specific retrieval of the exocytic SNARE Snc1p from early yeast endosomes. *Mol. Biol. Cell*. 11:23–38.

Luo, W., and A. Chang. 2000. An endosome-to-plasma membrane pathway involved in trafficking of a mutant plasma membrane ATPase in yeast. *Mol. Biol. Cell*. 11:579–592.

Marcusson, E.G., B.F. Horazdovsky, J.L. Cereghino, E. Gharakhanian, and S.D. Emr. 1994. The sorting receptor for yeast vacuolar carboxypeptidase Y is encoded by the *VPS10* gene. *Cell*. 77:579–586.

Meyer, C., D. Zizioli, S. Lausmann, E.L. Eskelinen, J. Hamann, P. Saftig, K. von Figura, and P. Schu. 2000. mu 1A-adaptin-deficient mice: lethality, loss of AP-1 binding and rerouting of mannose 6-phosphate receptors. *EMBO J.* 19:2193–2203.

Mumberg, D., R. Müller, and M. Funk. 1995. Yeast vectors for the controlled expression of heterologous proteins in different genetic backgrounds. *Gene*. 156:119–122.

Nothwehr, S.F., C.J. Roberts, and T.H. Stevens. 1993. Membrane protein retention in the yeast Golgi apparatus: dipeptidyl aminopeptidase A is retained by a cytoplasmic signal containing aromatic residues. *J. Cell Biol.* 121:1197–1209.

Nothwehr, S.F., E. Conibear, and T.H. Stevens. 1995. Golgi and vacuolar membrane proteins reach the vacuole in *vps1* mutant yeast cells via the plasma membrane. *J. Cell Biol.* 129:35–46.

Nothwehr, S.F., N.J. Bryant, and T.H. Stevens. 1996. The newly identified yeast *GRD* genes are required for retention of late-Golgi membrane proteins. *Mol. Cell. Biol.* 16:2700–2707.

Nothwehr, S.F., P. Bruinsma, and L.S. Strawn. 1999. Distinct domains within Vps35p mediate the retrieval of two different cargo proteins from the yeast prevacuolar/endosomal compartment. *Mol. Biol. Cell*. 10:875–890.

Nothwehr, S.F., S.-A. Ha, and P. Bruinsma. 2000. Sorting of yeast membrane proteins into an endosome-to-Golgi pathway involves direct interaction of their cytosolic domains with Vps35p. *J. Cell Biol.* 151:297–309.

Orlean, P., M.J. Kuranda, and C.F. Albright. 1991. Analysis of glycoproteins from *Saccharomyces cerevisiae*. *Methods Enzymol.* 194:682–697.

Owen, D.J., B.M. Collins, and P.R. Evans. 2004. Adaptors for clathrin coats: structure and function. *Annu. Rev. Cell Dev. Biol.* 20:153–191.

Payne, G.S., and R. Schekman. 1989. Clathrin: a role in the intracellular retention of a Golgi membrane protein. *Science*. 245:1358–1365.

Pelham, H.R. 1998. Getting through the Golgi complex. *Trends Cell Biol.* 8:45–49.

Pelham, H.R. 2004. Membrane traffic: GGAs sort ubiquitin. *Curr. Biol.* 14:R357–R359.

Puertollano, R., N.N. van der Wel, L.E. Greene, E. Eisenberg, P.J. Peters, and J.S. Bonifacino. 2003. Morphology and dynamics of clathrin/GGA1-coated carriers budding from the trans-Golgi network. *Mol. Biol. Cell*. 14:1545–1557.

Reggiori, F., and H.R. Pelham. 2001. Sorting of proteins into multivesicular bodies: ubiquitin-dependent and -independent targeting. *EMBO J.* 20:5176–5186.

Santos, B., and M. Snyder. 1997. Targeting of chitin synthase 3 to polarized growth sites in yeast requires Chs5p and Myo2p. *J. Cell Biol.* 136:95–110.

Scott, P.M., P.S. Bilodeau, O. Zhdankina, S.C. Winistorfer, M.J. Hauglund, M.M. Allaman, W.R. Kearney, A.D. Robertson, A.L. Boman, and R.C. Piper. 2004. GGA proteins bind ubiquitin to facilitate sorting at the trans-Golgi network. *Nat. Cell Biol.* 6:252–259.

Seaman, M.N. 2005. Recycle your receptors with retromer. *Trends Cell Biol.* 15:68–75.

Seeger, M., and G.S. Payne. 1992. Selective and immediate effects of clathrin heavy chain mutations on Golgi membrane protein retention in *Saccharomyces cerevisiae. J. Cell Biol.* 118:531–540.

Sharrocks, A.D. 1994. A T7 expression vector for producing N- and C-terminal fusion proteins with glutathione S-transferase. *Gene*. 138:105–108.

Sikorski, R.S., and P. Hieter. 1989. A system of shuttle vectors and yeast host strains designed for efficient manipulation of DNA in *Saccharomyces cerevisiae. Genetics*. 122:19–27.

Sipos, G., J.H. Brickner, E.J. Brace, L. Chen, A. Rambourg, F. Kepes, and R.S. Fuller. 2004. Soi3p/Rav1p functions at the early endosome to regulate endocytic trafficking to the vacuole and localization of TGN transmembrane proteins. *Mol. Biol. Cell*. 15:3196–3209.

Spelbrink, R.G., and S.F. Nothwehr. 1999. The yeast *GRD20* gene is required for protein sorting in the *trans*-Golgi network/endosomal system and for polarization of the actin cytoskeleton. *Mol. Biol. Cell*. 10:4263–4281.

Spormann, D.O., J. Heim, and D.H. Wolf. 1991. Carboxypeptidase yscS: gene structure and function of the vacuolar enzyme. *Eur. J. Biochem.* 197:399–405.

Subramanian, S., C.A. Woolford, and E.W. Jones. 2004. The Sec1/Munc18 protein, Vps33p, functions at the endosome and the vacuole of *Saccharomyces cerevisiae*. *Mol. Biol. Cell*. 15:2593–2605.

Valdivia, R.H., D. Baggot, J.S. Chuang, and R. Schekman. 2002. The yeast clathrin adaptor protein complex 1 is required for the efficient retention of a subset of late Golgi membrane proteins. *Dev. Cell*. 2:283–294.

Vida, T.A., and S.D. Emr. 1995. A new vital stain for visualizing vacuolar membrane dynamics and endocytosis in yeast. *J. Cell Biol.* 128:779–792.

Wach, A., A. Brachat, R. Pohlmann, and P. Philippsen. 1994. New heterologous modules for classical of PCR-based gene disruptions in *Saccharomyces cerevisiae. Yeast*. 10:1793–1808.

Yeung, B.G., H.L. Phan, and G.S. Payne. 1999. Adaptor complex-independent clathrin function in yeast. *Mol. Biol. Cell*. 10:3643–3659.

Ziman, M., J.S. Chuang, and R.W. Schekman. 1996. Chs1p and Chs3p, two proteins involved in chitin synthesis, populate a compartment of the *Saccharomyces cerevisiae* endocytic pathway. *Mol. Biol. Cell*. 7:1909–1919.